Kinetics and Product Formation during the Photooxidation of Butanol on Atmospheric Mineral Dust

M. Ponczek, C. George

KINETICS AND PRODUCT FORMATION DURING THE PHOTOOXIDATION OF BUTANOL ON ATMOSPHERIC MINERAL DUST

Milena Ponczek and Christian George*

Univ Lyon, Université Claude Bernard Lyon 1, CNRS, IRCELYON, F-69626, Villeurbanne, France

*correspondence to: christian.george@ircelyon.univ-lyon1.fr

Abstract

Mineral dust particles have photochemical properties that can promote heterogeneous reactions on their surfaces and therefore alter atmospheric composition. Even though dust photocatalytic nature has received significant attention recently, most studies have focused on inorganic trace gases. Here we investigated how light changes the chemical interactions between butanol and Arizona test dust, a proxy for mineral dust, under atmospheric conditions. Butanol uptake kinetics were measured, exploring the effects of UV light irradiation intensity (0 – 1.4 mW/cm), relative humidity (0 – 10%), temperature (283 – 298 K), and butanol initial concentration (20 – 55 ppb). The composition of the gas phase was monitored by a high-resolution proton-transfer-reaction mass spectrometer (PTR-ToF-MS) operating in H_3O^+ mode. Water was observed to play a significant role, initially reducing heterogeneous processing of butanol, but enhancing reaction rates once it evaporated. Gas phase products were identified, showing that surface reactions of adsorbed butanol led to the emission of a variety of carbonyl containing compounds. Under actinic light these compounds will photolyze and produce hydroxyl radicals, changing dust processing from a sink of VOC into a source of reactive compounds.

1 - Introduction

Every year, large amounts of mineral dust are emitted into the atmosphere and transported over several kilometers before being deposited. For instance, Kaufman and coworkers estimated that 240 ± 80 Tg of dust are transported annually from Africa to the Atlantic Ocean, and of these, 50 Tg arrives in the Amazon Basin.[1] During their lifetime in the troposphere, dust particles undergo physical interactions, including absorbing and scattering light, which influences radiative forcing and global albedo,[2] and inducing chemical reactions when acting as a substrate for the conversion or scavenging of various trace gases.[3] Heterogeneous reactions of atmospheric relevant trace gases on mineral aerosols have received more attention lately, and the uptake of a few reactive gases by mineral aerosols has been studied using a variety of experimental approaches. For instance, the uptake kinetics of inorganic compounds such as NO_2, HNO_3, N_2O_5, O_3, SO_2,[4–7] as well as some organics [8,9] were investigated on mineral dust and various proxies. However, few studies have explored the effect of irradiation on the uptake.

Suspended dust particle composition varies depending on its sources location and may contain variable amounts of semiconductor metal oxides that show photocatalytic activity, such as TiO_2 and Fe_2O_3, whose application in wastewater and air treatment have been extensively studied.[10–13] Recently, the photocatalytic nature of dust particles has been suggested and discussed.[14,15] However, up to now, the most investigations focused on inorganic compounds such as ozone,[16] nitrogen dioxide,[17] sulfur dioxide,[18,19] and hydrogen peroxide,[20] and little is known about mineral dust photoreactivity towards volatile organic compounds (VOC). [21,22]

To assess the importance of photocatalytic transformations of volatile organic compounds on mineral dust, we investigated the uptake kinetics of butanol on Arizona test dust (ATD). We performed experiments under dark and illuminated conditions and measured uptake coefficients as a function of several experimental parameters, including initial VOC concentration, relative humidity, external temperature, and light intensity. Additionally, we analyzed the gas phase products,

evaluating the role of dust and the influence of light, whose effects are quantified and discussed.

Butanol was selected as a proxy for small alcohols (and/or oxygenated VOCs; OVOC) that are abundant in the atmosphere. OVOCs are generally emitted directly by anthropogenic sources, biogenic sources, or produced from the degradation of other VOCs (hydrocarbon oxidation). Butanol, specifically, is an alcohol that does not absorb light in the UV or visible regions, but its incomplete oxidation products can generate photochemically active radicals.

2 - Experimental

Coated wall flow tube

Experiments were performed in a horizontal coated wall flow tube reactor described in detail previously.[23] The temperature was maintained constant during each experiment by circulating thermostatically controlled water around an outer jacket. Dust was coated on the inner surface of a removable Pyrex insert (id 0.55 cm, length 20 cm), which fit within a larger tube, providing good contact with the jacket. Seven actinic lamps (Phillips 20 W) surrounded the reactor and could be switched on or off to modify the light intensity between 0 and 1.4 mW/cm² (see Supplementary Information, Figure S1) measured at the outer surface of the reactor. It is important to highlight that in this layout, UV light was irradiated from the back of the coatings, which were relatively thin (µm) with a maximum absorption of 15% i.e., the film is mostly homogeneously illuminated. Also, our approach does not consider light scattering in the dust film. However, Dupart et al[24] showed that this approach led, nevertheless, to similar uptake kinetics measured in more complex aerosol flow tube experiments where such limitations do not exist. Therefore, we believe that the light intensity measured is appropriate for the experiments described herein.

All experiments were carried out at atmospheric pressure using filtered dry air as a carrier gas at a total flow of 200 mL min^{-1}, except when stated otherwise. For humid experiments, water vapor

was introduced into the reactor by bubbling air through a thermostated gas bubbler filled with deionized water. Humidity and temperature were monitored by a SP UFT75 sensor.A schematic overview of the experimental setup is given in Figure S3. Gas phase butanol was generated using a calibrated permeation tube (*Dynacal*® - permeation rate 100 ng/min at 60 ºC) placed in a temperature-controlled permeation device (VICI Metronics Dynacalibrator, Model 150).

Gas phase analysis

The coated wall flow tube was coupled to a high-resolution proton transfer reaction time of flight mass spectrometer (SRI-PTR-TOF-MS 8000 from Ionicon Analytik GmbH – Innsbruck, Austria) enabling on-line monitoring of the disappearance of butanol and the identification and quantification of products. The instrument continuously sampled 50 sccm at the flow tube outlet and its inlet temperature was 60 °C. Spectra were collected at a time resolution of 3.2 s. All measurements were performed using the following parameters: source current of 4.6 mA, drift voltage of 600 V, drift temperature of 60 °C, and a drift pressure of 2.42 mbar. E/N was about 125 Td (1 Td = 10^{-17} V cm^2). All results presented here were acquired using the H_3O^+ ionization mode as the reaction rates and fragmentation patterns for OVOCs such as alcohols, aldehydes, ketones, etc., have been extensively studied and documented.[25–28]

Ideally, the proton transfer reaction should provide soft ionization resulting in very little or no fragmentation of compounds. However, in practice, fragmentation is observed. Fragmentation patterns for small OVOCs have already been studied, but it may be altered depending on the actual experimental conditions (for example, humidity) and instrument settings.[29] Therefore, fragmentation patterns of the main products were examined by measuring the signals of vaporized liquid standards under the same experimental conditions. Details about this procedure are available in the Supplementary Information.

Film Preparation

Arizona Test Dust (ATD) was used as provided by Powder Technology Inc. without further pretreatment. The ATD Brunauer – Emmett – Teller surface area (BET) is 4.2 ± 0.012 m^2 g^{-1} as measured with a Micromeritics Tristar 3000, with particles having an average grain size of 4.08 ± 2.91 μm.

ATD suspensions in ethanol were prepared to facilitate coating the inner surface of the Pyrex tube insert. These suspensions were sonicated for 10 minutes and then dripped into the insert, which was rotated to produce a uniform film. Once coated, the excess solution was allowed to flow out and the tube was dried by flowing nitrogen through it. This step was repeated few times until a visually homogeneous film was obtained. Finally, the insert was placed in an oven to dry at 60 °C for 24 h. After drying, all tubes were weighed, and the mass of ATD films varied from 20 to 150 mg.

Uptake Experiments

Butanol loss was measured as a function of the movable injector position, that is, interaction time between the VOC and dust surface. In a typical experiment, a freshly coated tube was placed in the reactor and the injector was set to bypass the reactor, so that no surface was exposed to the gas flow (position 0). The flow of butanol was then established and its concentration monitored. When it was constant, lights were switched on. After 60 minutes, the uptake measurements started by moving the injector stepwise (steps of 2 cm), exposing the ATD surface for 10 minutes. The injector was then reset to position 0 for another 10 minutes. The procedure was repeated until the entire length of the coated tube was exposed, which is equivalent to 10 positions of 2 cm each.

The decay of gas phase butanol obeyed first order kinetics according to:

$$\ln\frac{C(0)}{C(t)} = k_{obs}t \qquad [1]$$

C(0) and C(t) are the inlet and outlet concentrations of butanol after a reaction time (t), and k_{obs} is the measured first order rate constant. The uptake coefficient can then be calculated according to:

$$\gamma = \frac{4\,k_{obs}}{\langle v \rangle}\,\frac{V}{S_{surf}} \qquad [2]$$

where V is the total volume of the reactor, S_{surf} is the surface area exposed to the gas, and ‹v› is average molecular velocity. For a cylindrical flow tube, the geometric uptake coefficient is given by:

$$\gamma_{geo} = \frac{2r}{\langle v \rangle}\,k_{obs} \qquad [3]$$

where r is the radius (r_{tube} = 0.55 cm).

It is worth noting that the uptake coefficients reported here are at steady state, reached after 10 minutes of exposure, and not the initial uptake coefficients usually reported in the literature.[4]

Diffusion correction

Uptake was corrected for diffusion effects that may form axial and radial concentration profiles along the reactor, limiting the reaction rate. The method used, proposed by Cooney-Kim-Davis and derived by Murphy and co-workers,[30] assumes that in the boundary condition the analyte is adsorbed or reacts with some characteristic probability on each wall collision, which is the corrected uptake coefficient. We solved the differential equation numerically, as proposed by Li et al.,[31] where the corrected uptake coefficient is given as function of the transmittance (C/Co).

3 – Results and Discussion

Butanol Uptake Kinetics

For a solid film, the reactive surface area may be larger than the geometric surface area due to the presence of multiple layers of particles and/or because of the existence of pores. In the case of a fully accessible internal surface, the specific surface area can be used for the uptake calculations. Therefore, butanol uptake coefficients were measured as a function of dust film mass (Figure S3a). For these measurements, different fresh films of ATD were tested while other conditions were kept constant. The uptake coefficient increased linearly with the mass of the film, indicating that the entire inner surface is participating in the uptake process.[4] Therefore, mass-dependent γ_{geo} uptake coefficients were corrected by the BET surface area of the samples according to:

$$\gamma_{BET} = \gamma_{Geo} \frac{S_{surf}}{S_{BET}\, m_{film}} \quad [4]$$

where S_{BET} is the BET surface area and m_{film} is the mass coated in the sample holder tube. The BET-corrected uptake coefficients, reported below, were observed to be independent of the actual mass of the film (Figure S3b).

Uptake rates were measured for different initial (inlet) concentrations of butanol and were observed to decrease from 5.3×10^{-7} to 2.2×10^{-7} when the concentration increases from 20 to 55 ppb (Figure S4). For an initial concentration of 800 ppb (± 160 ppb) of butanol, uptake could not be detected, due to very rapid surface saturation. Initial uptake coefficients tend to be independent of concentration when all active sites on the fresh surface are available for adsorption/reaction.[7,32] El Zein et al.[20] reported no concentration dependence for the initial uptake coefficient, whereas an inverse dependence on initial H_2O_2 concentration was observed for steady state uptake. Nicolas et al.,[16] using a similar experimental apparatus, also reported that both dark and irradiated uptake kinetics on titanium dioxide decreased inversely to initial ozone mixing ratio.

When the temperature increased from 283 to 298 K, the uptake coefficient decreased from 1.2 x 10^{-6} to 1.8 x 10^{-7}, which is approximately one order of magnitude (Figure S5). The reactive uptake coefficient reported herein represents the overall kinetics of the heterogeneous process, and therefore encompasses both chemical reactions and physical adsorption. Adsorption is an exothermic phenomenon favored by a decrease in temperature.[33] Thereby, the temperature dependence suggests the importance of adsorption/desorption in the butanol uptake mechanism, even under reactive conditions. A similar dependence was previously reported for other VOCs.[32, 34]

Humidity also has a strong influence on the uptake kinetics of butanol onto ATD (Figure S6). At 10% relative humidity, the uptake coefficient is 6% of the value measured under dry conditions, suggesting that water and butanol compete for available sites on the surface of ATD. To better understand the influence of relative humidity on butanol uptake, an ATD film was successively exposed to different relative humidity levels under dark conditions. First, the tube was exposed to air and butanol (20 ppb) under dry conditions, and the disappearance of butanol was recorded. Then, butanol flow was turned off and the tube was left under air until butanol was not detected. Thereafter, butanol flow was resumed and the sample was exposed to the VOC with 2%, 5%, and 10% moisture. Between each relative humidity level, the sample was left under dry air flow for evacuation. The presence of water vapor in the feed stream significantly reduced butanol surface adsorption capacities (Figure S7). Surface saturation was faster at higher water vapor contents, up to 10% relative humidity, no change in butanol concentration was observed.

The uptake of water onto mineral particles has been studied by several authors and recently reviewed.[35] However few studies have focused on the competitive uptake of water and other trace gases, particularly under irradiation. For pure TiO_2, relative humidity has a positive effect up to about 30% relative humidity, as observed by Sassine et al.,[36] who reported that the uptake of formaldehyde increased from 6% to 30% relative humidity, and decreased at higher humidities. The influence of humidity seems to vary depending on the combination of trace gas and mineral studied, and results are often controversial. Under dark conditions using ATD and other realistic dust, regardless of the

trace gas studied, relative humidity has been found to have a negative influence on gas uptake. [19, 32, 37, 38] Our results show that the presence of light did not change this negative trend for butanol uptake.

In terms of competition between butanol and water for available surface sites, water molecules are smaller and faster, giving them an advantage over butanol molecules. Regarding the affinity between the mineral surface and water molecules, Gustafson and coworkers[39] noted a difference between ATD and $CaCO_3$ isotherms in the sub-monolayer range, demonstrating stronger water-ATD interactions compared to $CaCO_3$. They proposed that the difference might be due to the higher electronegativity of Si which increases the polarity of the –OH group, resulting in a stronger H-bond in the ATD. Furthermore, water adsorption capacity is related to other characteristics such as the mineral composition, cation hydration energies, presence of swellable clay minerals, porosity, etc.[40]

Interestingly, the system shows a hysteresis. When the ATD film was exposed to decreasing levels of relative humidity under irradiation, butanol uptake increased more rapidly than was observed for a freshly humidified surface (Figure 1). That is, water condensation may first reduce heterogeneous processing, but its evaporation may afterwards change the surface characteristics to enhance its reactivity. Water uptake measurements on ATD have shown that one monolayer of water is developed at about 11% relative humidity.[39] In going from dry to slightly humid conditions, adsorbed water molecules dissociate leaving OH groups on the surface. By increasing relative humidity, once surface is fully hydroxylated, extra water molecules will be accommodated in outer layers via hydrogen bonds.[41] Those surface OH groups can form OH radicals under dry conditions and illumination, providing an additional pathway for butanol oxidation.

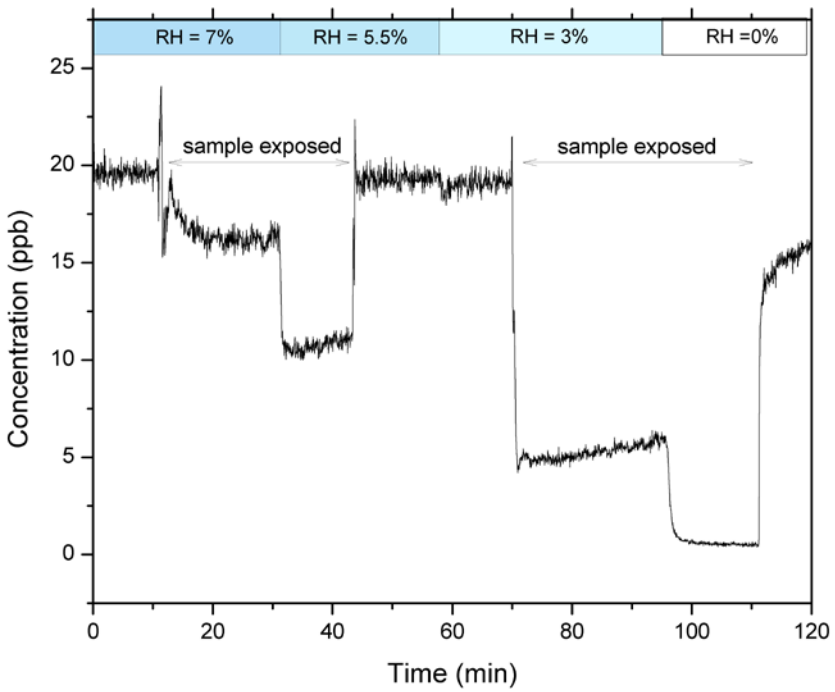

Figure 1: Decreasing relative humidity (RH) and successively exposing the sample surface to butanol and H_2O vapor. For butanol initial concentration of 20 ppb, temperature = 20 °C, 7 lamps, mass of ATD = 69 mg.

Our experimental setup allowed switching between 0 and 7 lamps in different geometrically symmetrical configurations. Each lamp emits UV-A radiation in the wavelength range from 300 to 420 nm, with a maximum around 350 nm. Figure S8 shows the systematic increase of the uptake coefficient as a function of UV light irradiance. The dark uptake coefficient is 5 times less than the light uptake coefficient for irradiation with 7 lamps. This gives clear evidence of the photochemical nature of the interactions between butanol (which does not absorb within this wavelength region) and ATD (which semiconductor content is activated by light). This is in agreement with previous studies which also observed photo-enhanced uptake for inorganic compounds over different mineral dust proxies.[16-20, 37, 38] However, few similar studies on organic compounds are available.[21]

Photochemistry of butanol on ATD surface

The uptake (loss) of butanol was accompanied by the formation of a variety of gas phase products (Figure 2). Major products were observed at m/z 45.033 ($C_2H_5O^+$), 31.017 (CH_3O^+), 59.049 ($C_3H_7O^+$), 33.033 (CH_5O^+), 69.069 ($C_5H_9^+$), 115.111 ($C_7H_{15}O^+$), and five other minor products were detected at very low concentrations (below 0.1 ppb) at 83.085 ($C_6H_{11}^+$), 87.080 ($C_5H_{11}O^+$), 97.101 ($C_7H_{13}^+$), 111.116 ($C_8H_{15}^+$), and 129.127 ($C_8H_{17}O^+$). Products identification is detailed in Table 1. It is interesting to note that fragments with m/z greater than butanol were also detected (for instance m/z 69.069 and m/z 115.111), indicating the possibility of dimerization or recombination of intermediates. It should be noted that m/z 31.017 is here assigned to formaldehyde, although other compounds may interfere at this m/z, as discussed by Schirpp et al. and Inomata et al.[42, 43]. No product formation was observed in the dark.

Table 1: Product identification and m/z to molecules assignments.

Major Products			**Minor Products**		
m/z	**Formula**	**Compound**	**m/z**	**Formula**	**Compound**
45.033	$C_2H_5O^+$	Acetaldehyde	**83.085**	$C_6H_{11}^+$	fragment Hexanal
31.017	CH_3O^+	Formaldehyde / fragment Propanal	**87.080**	$C_5H_{11}O^+$	Pentanal
59.049	$C_3H_7O^+$	Propanal/ Acetone	**97.101**	$C_7H_{13}^+$	fragment Heptanal
33.033	CH_4O^+	Metanol	**111.116**	$C_8H_{15}^+$	fragment Octanal
69.069	$C_5H_9^+$	fragment Octanal / Pentanal	**129.127**	$C_8H_{17}O^+$	Octanal
115.111	$C_7H_{15}O^+$	Heptanal			

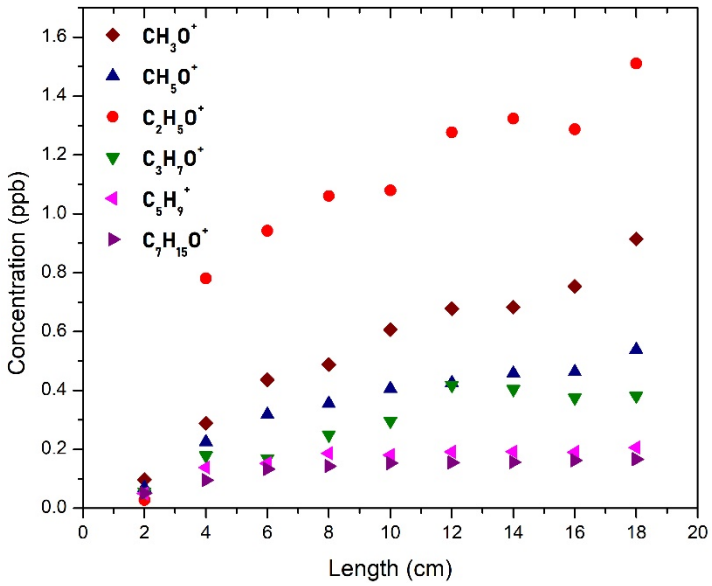

Figure 2: Product concentration profile for each position/residence time along the reactor. For initial butanol concentration of 20 ppb, dry conditions, T = 20 °C, 7 lamps, mass of ATD = 110 mg.

To explore whether these products are arising from "freshly" up taken butanol or from adsorbed molecules, a film was exposed to gas phase butanol in the dark until surface saturation (i.e., constant butanol signal). Maintaining the butanol flow throughout the reactor, the lights were then switched on and off in the following sequence: 1) 30 minutes two lamps on; 2) 30 minutes four lamps on; 3) 1 hour all lamps off; 4) 30 minutes 6 lamps on. We observed (see Figure 3) production of different compounds (CH_3O+, C_2H_5O+, C_3H_7O+, C_5H_9+, and $C_7H_{15}O+$) immediately after the lights were turned on, with increasing intensity at higher light fluxes. Nevertheless, there was no drop in the gas phase butanol concentration, suggesting that products were formed from butanol already adsorbed on the surface. Product formation was quantified (subtracting the background value from the concentration during irradiation) for each round of illumination (number of lamps switched on; Figure 4). Although only major products are shown in Figure 3 and Figure 4, the same minor products listed in Table S3 were also present. Figure 4 clearly demonstrates that irradiation enhanced product formation. It is known that photocatalytic reaction rates are proportional to the radiant flux for low/moderate illumination intensities.[44] Chapuis et al.[45] also observed lower product concentrations at lower light intensities, other factors being equal, for the photocatalytic oxidation (PCO) of n-

butanol.

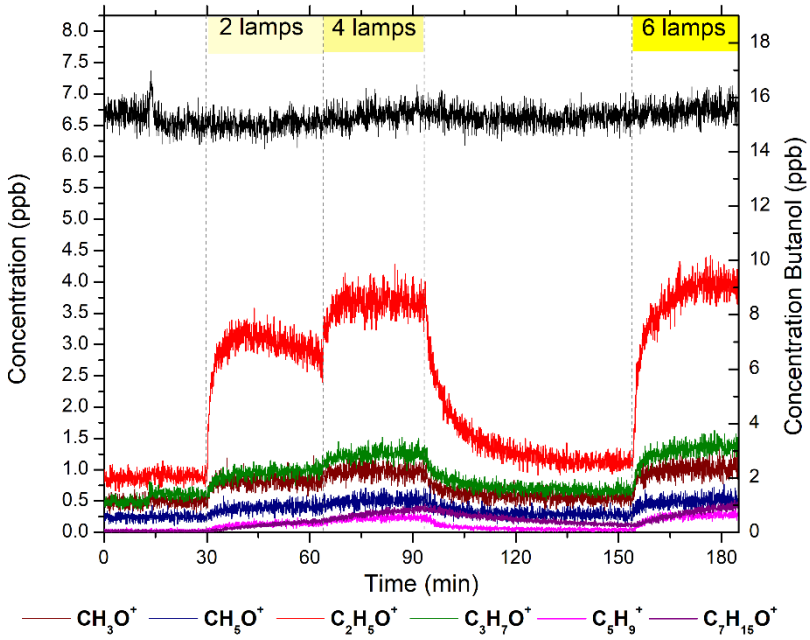

Figure 3: Saturation experiment: Concentration profiles for butanol (right scale) and main products over butanol-saturated ATD surface for different irradiation intensities (2, 4, and 6 lamps, indicated by bars above the graph). Experimental conditions were: Air flow rate 200 ml/min, dry conditions, T = 20 °C, mass of ATD = 35 mg.

Concerning the study of alcohols under atmospheric simulated conditions onto different mineral proxies, mainly small aldehydes, ketones, and carboxylic acids were reported as products. Styler and Donaldson[21] studied the photooxidation of isopropanol and n-propanol over TiO_2 films in a Knudsen cell, operated at much lower pressure than in the current investigation, and identified acetone and propionaldehyde, respectively, as main products. The same authors, Styler, Myers, and Donaldson,[46] studied the photooxidation of fluorotelomer alcohols onto Mauritanian sand and volcanic ashes and found aldehydic products in the gas phase and perfluorinated carboxylic acids as sorbed products. Recently, Romanias and coworkers[32] also studied the photochemistry of isopropanol on Gobi natural dust under pure air, reporting the formation of acetone, formaldehyde, acetic acid, and acetaldehyde as products when the dust was illuminated.

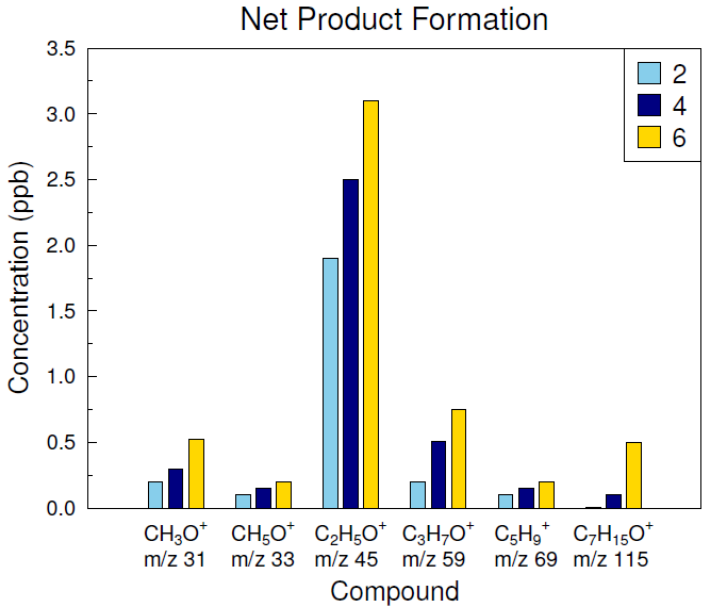

Figure 4: Net product formation of major products for different light intensities during the saturation experiment (Figure 3). The number of lamps is represented by bar color as indicated in the legend.

Most of the available literature for alcohols, and specifically butanol, investigates photocatalytic oxidation (PCO) on TiO_2, with the goal of optimizing conditions to mineralize the organic compound. Yao and Feilberg[47] quantified product formation for the photocatalytic degradation of 52 ppb of n-butanol through TiO_2-coated ceramic filters, reporting acetaldehyde, butyraldehyde, propionaldehyde/acetone, ethanol, formic acid, acetic acid, and formaldehyde as potential byproducts. They pointed out, however, that the observed products accounted for only a fraction of the reactant consumption, suggesting that butanol could be directly degraded producing CO_2 and water.

In our case, the total yield (sum of the yield of all detected products) is around 30 – 40%, implying that either all of the adsorbed butanol is not converted into products, or some butanol is converted into non-volatile products that accumulate on the surface or yet is mineralized to CO_2 and water. Butanal can be expected to be one of the first intermediates from the butanol oxidation, it is

therefore interesting to note that we did not detect it. It was however detected in studies investigating the oxidation on pure TiO_2 at much higher concentrations than ours.[47–51] In addition to butanal, propionaldehyde, acetaldehyde, 1-propanol, and ethanol were also found by those authors. It is worthwhile to note that all of these studies investigated oxidation on pure TiO_2 at much higher concentrations than used in this study. Nevertheless, this study generally agrees with previous reports that, mineral dust (ATD containing 2.0 – 5.0 wt% Fe_2O_3 and 0.5 – 1 wt% TiO_2) can promote photooxidation of an organic compound on its surface similar to pure semiconductors such as TiO_2.

Gas phase products give some insight into the butanol degradation mechanism under our experimental conditions. We propose that during photooxidation adsorbed butanol is first directly oxidized to an aldehyde by photo-generated holes or OH radicals from residual water on the surface.

$$TiO_2 + h\upsilon \leftrightarrows h^+_{vb} + e^-_{cb} \quad [5]$$

$$H_2O_{(ads)} + h^+_{vb} \rightarrow {}^{\bullet}OH + H^+ \quad [6]$$

$$R - CH_2 - OH_{(ads)} + h^+ (or\ {}^{\bullet}OH) \rightarrow R - CHO + H^+ \quad [7]$$

The process then continues via a series of complex reactions, which are expected to be similar to those proposed by other authors,[48, 52, 53] with aldehydes being converted to shorter chain aldehydes and/or alcohols.

As presented by Ye et al.,[53] aldehydes are oxidized via two pathways, either through the C(n) acid, or by direct conversion to the C(n-1) aldehyde. No acids were detected here, which may be due to their lower volatility or their high affinity for the dust surface (and tubing). Alcohols such as propanol and ethanol can also remain adsorbed on dust surface.[45] A global mechanism is suggested in Figure 5. In general, we can say:

$$R - OH + h^+ (or\ \cdot OH) \rightarrow R - CHO \xrightarrow{O_2} R - COOH + h^+ \rightarrow \begin{matrix} R_{(n-1)}CHO \\ R_{(n-1)} - OH \end{matrix} \quad [8]$$

Some studies highlight the contribution of superoxide radical and other radical species derived from oxygen.[52, 54] The superoxide radical may contribute, for instance, to charge separation (between e_{cb}^{-} and h_{vb}^{+}). Molecular O_2 is also very important, as it can directly oxidize the aldehyde to an acid[48] or react with alkyl radicals,[52] forming a hydroxylated peroxyl radical and HOO• radicals. In anhydrous systems, O_2 is the active oxidizing species, and its ionosorbates are the only negatively charged species able to react with holes. [33]

$$O_{2\,(g)} \rightarrow 2\,O_{ads} \quad [9]$$

$$O_{ads} + e^{-} \rightarrow O_{ads}^{-} \quad [10]$$

$$O_{ads}^{-} + h^{+} \rightarrow O_{ads}^{*} \quad [11]$$

Additionally, intermediary reactions in the oxidation mechanism may lead to the formation of radicals, resulting in the propagation of chain reactions[52] involving O_2.[54] Recombination of radicals is then likely to occur, resulting in products of higher molar mass than the initial compound.

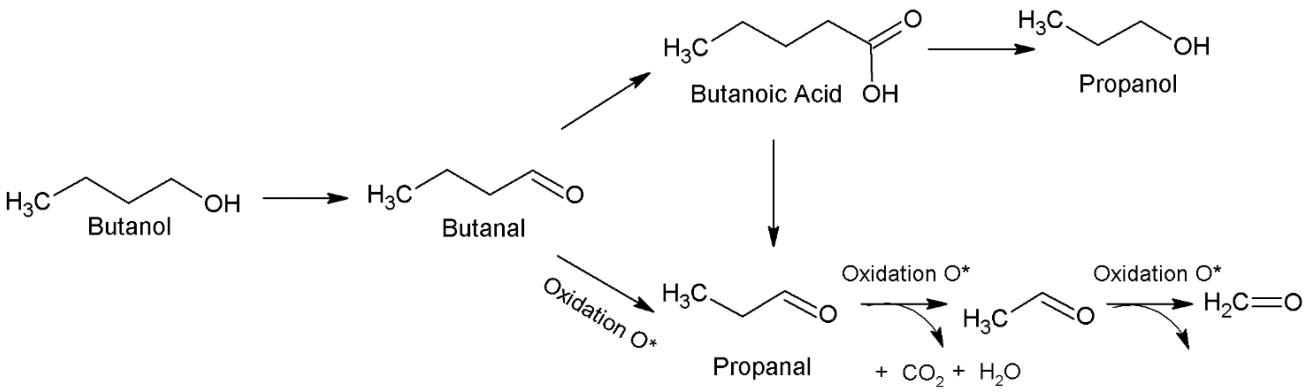

Figure 5: Suggested mechanism for butanol photooxidation on ATD's surface.

Carbonyl compounds were the predominant products observed in the gas phase. Aldehydes and ketones absorb at UV-Vis wavelengths (>290 nm), acting as radical precursors for further photochemical reactions. On the other hand, alcohols, including butanol, do not absorb light at these

wavelengths and therefore generally have longer lifetimes in the troposphere.[55] We emphasize that mineral dust plays an important role not only acting as a scavenger for alcohol molecules, but also in converting them into more reactive species.

Atmospheric Implications

We presented the effect of ambient conditions such as temperature, relative humidity, and light intensity on an oxygenated organic compound uptake on realistic mineral dust particles. Uptake was maximized at low temperature and low humidity.

We estimated the lifetime of butanol due to its heterogeneous photooxidation on mineral dust surfaces. The calculation used the first order rate constant under atmospheric conditions i.e., with the uptake coefficient measured at 20 ppbv of butanol, for dry conditions, at 20° C under a real UV-A (315-400 nm) irradiance, determined using the Quick TUV model, for latitude of 40° North at noon during equinox day, or solar zenith angle of 40° . For very high dust loadings (surface area density of 0.052 $m^2 m^{-3}$), the butanol lifetime was found to be 1.48 days whereas for regular clean days (surface area density of $1x10^{-4}$ $m^2 m^{-3}$) it was 770 days. By comparison, the butanol lifetime due to OH radical reaction is estimated as 1.4 days.[55] As a consequence, this butanol removal pathway can only be effective in a dust plume.

More importantly, the photochemistry described here occurs on illuminated mineral dust, with adsorbed organic compounds typically being oxidized to shorter and more volatile products. Butanol, for instance, will produce aldehydes such as formaldehyde, acetaldehyde, and propionaldehyde which are potential sources of atmospheric radicals. More complex products (e.g., dimers of reaction intermediates) were also formed in small amounts. In other words, mineral dust can be regarded as a reservoir for such compounds, transporting pollution for source regions to remote places and may transport, where tens of pptv of aldehydes may be a significant contribution to their actual concentrations. Overall, mineral dust is not inert and opens new photochemical pathways that so far

have not been considered in current atmospheric models.

Acknowledgements

The authors gratefully acknowledge the Brazilian National Council for Scientific and Technological Development−CNPq, Brazil for the financial support (PhD fellowship of M. P.)

Supporting Information

Lamp calibrations (total irradiance for different configuration of lamps) are presented in Figures S1 and Table S1. A schematic overview of the experimental setup is given in Figure S2. Dependence of geometric uptake coefficient on butanol and the BET uptake coefficients are shown in Figure S3a and S3b, respectively. BET uptake coefficients as a function of butanol concentration, reactor temperature, relative humidity, and number of lamps are shown in Figure S4, S5, and S6, S8. Butanol loss upon exposing an ATD film to different relative humidity levels under dark conditions is presented in Figure S7. Details about product identification and PTR-MS standards are also given in the SI in Figure S9 and Tables S2 and S3.

388 **References**

389 (1) Kaufman, Y. J. Dust Transport and Deposition Observed from the Terra-Moderate
390 Resolution Imaging Spectroradiometer (MODIS) Spacecraft over the Atlantic Ocean. *J.*
391 *Geophys. Res.* **2005**, *110* (D10), D10S12.

392 (2) Sa'id, R. S. Dust Aerosols And Climate: A Brief Review. *Adv. Sci. Technol.* **2012**, *6* (2),
393 115–122.

394 (3) Usher, C. R.; Michel, A. E.; Grassian, V. H. Reactions on Mineral Dust. *Chem. Rev.* **2003**,
395 *103* (12), 4883–4939.

396 (4) Underwood, G. M.; Li, P.; Usher, C. R.; Grassian, V. H. Determining Accurate Kinetic
397 Parameters of Potentially Important Heterogeneous Atmospheric Reactions on Solid Particle
398 Surfaces with a Knudsen Cell Reactor. *J. Phys. Chem. A* **2000**, *104* (4), 819–829.

399 (5) Seisel, S.; Borensen, C.; Vogt, R.; Zellner, R. Kinetics and Mechanism of the Uptake of
400 N2O5 on Mineral Dust at 298 K. *Atmos. Chem. Phys.* **2005**, *5* (12), 3423–3432.

401 (6) Hanisch, F.; Crowley, J. N. Ozone Decomposition on Saharan Dust: An Experimental
402 Investigation. *Atmos. Chem. Phys.* **2003**, *3* (1), 119–130.

403 (7) Adams, J. W.; Rodriguez, D.; Cox, R. A. The Uptake of SO_2 on Saharan Dust: A Flow Tube
404 Study. *Atmos. Chem. Phys.* **2005**, *5* (10), 2679–2689.

405 (8) Carlos-Cuellar, S.; Li, P.; Christensen, A. P.; Krueger, B. J.; Burrichter, C.; Grassian, V. H.
406 Heterogeneous Uptake Kinetics of Volatile Organic Compounds on Oxide Surfaces Using a
407 Knudsen Cell Reactor: Adsorption of Acetic Acid, Formaldehyde, and Methanol on α-Fe 2 O
408 3 , α-Al 2 O 3 , and SiO 2. *J. Phys. Chem. A* **2003**, *107* (21), 4250–4261.

409 (9) Li, P.; Perreau, K. A.; Covington, E.; Song, C. H.; Carmichael, G. R.; Grassian, V. H.
410 Heterogeneous Reactions of Volatile Organic Compounds on Oxide Particles of the Most
411 Abundant Crustal Elements: Surface Reactions of Acetaldehyde, Acetone, and

412 Propionaldehyde on SiO 2 , Al 2 O 3 , Fe 2 O 3 , TiO 2 , and CaO. *J. Geophys. Res. Atmos.*
413 **2001**, *106* (D6), 5517–5529.

414 (10) Herrmann, J.-M. Heterogeneous Photocatalysis: Fundamentals and Applications to the
415 Removal of Various Types of Aqueous Pollutants. *Catal. Today* **1999**, *53* (1), 115–129.

416 (11) Alberici, R. M.; Jardim, W. F. Photocatalytic Destruction of VOCs in the Gas-Phase Using
417 Titanium Dioxide. *Appl. Catal. B Environ.* **1997**, *14* (1–2), 55–68.

418 (12) Litter, M. Heterogeneous Photocatalysis Transition Metal Ions in Photocatalytic Systems.
419 *Appl. Catal. B Environ.* **1999**, *23* (2–3), 89–114.

420 (13) Wang, N.; Zheng, T.; Zhang, G.; Wang, P. A Review on Fenton-like Processes for Organic
421 Wastewater Treatment. *J. Environ. Chem. Eng.* **2016**, *4* (1), 762–787.

422 (14) Chen, H.; Nanayakkara, C. E.; Grassian, V. H. Titanium Dioxide Photocatalysis in
423 Atmospheric Chemistry. *Chem. Rev.* **2012**, *112* (11), 5919–5948.

424 (15) George, C.; Ammann, M.; D'Anna, B.; Donaldson, D. J.; Nizkorodov, S. a. Heterogeneous
425 Photochemistry in the Atmosphere. *Chem. Rev.* **2015**, *115* (10), 4218–4258.

426 (16) Nicolas, M.; Ndour, M.; Ka, O.; D'Anna, B.; George, C. Photochemistry of Atmospheric
427 Dust: Ozone Decomposition on Illuminated Titanium Dioxide. *Environ. Sci. Technol.* **2009**,
428 *43* (19), 7437–7442.

429 (17) Ndour, M.; D'Anna, B.; George, C.; Ka, O.; Balkanski, Y.; Kleffmann, J.; Stemmler, K.;
430 Ammann, M. Photoenhanced Uptake of NO 2 on Mineral Dust: Laboratory Experiments and
431 Model Simulations. *Geophys. Res. Lett.* **2008**, *35* (5), L05812.

432 (18) Dupart, Y.; King, S. M.; Nekat, B.; Nowak, A.; Wiedensohler, A.; Herrmann, H.; David, G.;
433 Thomas, B.; Miffre, A.; Rairoux, P.; et al. Mineral Dust Photochemistry Induces Nucleation
434 Events in the Presence of SO2. *Proc. Natl. Acad. Sci. U. S. A.* **2012**, *109* (51), 20842–20847.

435 (19) Huang, L.; Zhao, Y.; Li, H.; Chen, Z. Kinetics of Heterogeneous Reaction of Sulfur Dioxide

on Authentic Mineral Dust: Effects of Relative Humidity and Hydrogen Peroxide. *Environ. Sci. Technol.* **2015**, *49* (18), 10797–10805.

(20) Zein, A. El; Romanias, M. N.; Bedjanian, Y. Heterogeneous Interaction of H2O2 with Arizona Test Dust. *J. Phys. Chem. A* **2014**, *118* (2), 441–448.

(21) Styler, S. a; Donaldson, D. J. Photooxidation of Atmospheric Alcohols on Laboratory Proxies for Mineral Dust. *Environ. Sci. Technol.* **2011**, *45* (23), 10004–10012.

(22) Styler, S. a.; Donaldson, D. J. Heterogeneous Photochemistry of Oxalic Acid on Mauritanian Sand and Icelandic Volcanic Ash. *Environ. Sci. Technol.* **2012**, *46* (16), 8756–8763.

(23) Ndour, M.; Conchon, P.; D'Anna, B.; Ka, O.; George, C. Photochemistry of Mineral Dust Surface as a Potential Atmospheric Renoxification Process. *Geophys. Res. Lett.* **2009**, *36* (5), L05816.

(24) Dupart, Y.; Fine, L.; D'Anna, B.; George, C. Heterogeneous Uptake of NO2 on Arizona Test Dust under UV-A Irradiation: An Aerosol Flow Tube Study. *Aeolian Res.* **2014**, *15* (2), 45–51.

(25) Spanel, P.; Smith, D. SIFT Studies of the Reactions of H3O+, NO+ and O2+ with a Series of Alcohols. *Int. J. Mass Spectrom. Ion Process.* **1997**, *167–168* (2), 375–388.

(26) Španěl, P.; Ji, Y.; Smith, D. SIFT Studies of the Reactions of H3O+, NO+ and O2+ with a Series of Aldehydes and Ketones. *Int. J. Mass Spectrom. Ion Process.* **1997**, *165–166*, 25–37.

(27) Španěl, P.; Smith, D. SIFT Studies of the Reactions of H3O+, NO+ and O2+ with Several Ethers. *Int. J. Mass Spectrom. Ion Process.* **1998**, *172* (3), 239–247.

(28) Smith, D.; Chippendale, T. W. E.; Španěl, P. Reactions of the Selected Ion Flow Tube Mass Spectrometry Reagent Ions H3O+ and NO+ with a Series of Volatile Aldehydes of Biogenic Significance. *Rapid Commun. Mass Spectrom.* **2014**, *28* (17), 1917–1928.

(29) de Gouw, J.; Warneke, C. Measurements of Volatile Organic Compounds in the Earth's

Atmosphere Using Proton-Transfer-Reaction Mass Spectrometry. *Mass Spectrom. Rev.* **2007**, *26* (2), 223–257.

(30) Murphy, D. M.; Fahey, D. W. Mathematical Treatment of the Wall Loss of a Trace Species in Denuder and Catalytic Converter Tubes. *Anal. Chem.* **1987**, *59* (23), 2753–2759.

(31) Li, G.; Su, H.; Li, X.; Kuhn, U.; Meusel, H.; Hoffmann, T.; Ammann, M.; Pöschl, U.; Shao, M.; Cheng, Y. Uptake of Gaseous Formaldehyde by Soil Surfaces: A Combination of Adsorption/desorption Equilibrium and Chemical Reactions. *Atmos. Chem. Phys.* **2016**, *16* (15), 10299–10311.

(32) Romanias, M. N.; Zeineddine, M. N.; Gaudion, V.; Lun, X.; Thevenet, F.; Riffault, V. Heterogeneous Interaction of Isopropanol with Natural Gobi Dust. *Environ. Sci. Technol.* **2016**, *50* (21), 11714–11722.

(33) Herrmann, J.-M. Active Agents in Heterogeneous Photocatalysis: Atomic Oxygen Species vs. OH.cntdot. Radicals: Related Quantum Yields. *Helv. Chim. Acta* **2001**, *84* (9), 2731–2750.

(34) Liu, Q.; Wang, Y.; Wu, L.; Jing, B.; Tong, S.; Wang, W.; Ge, M. Temperature Dependence of the Heterogeneous Uptake of Acrylic Acid on Arizona Test Dust. *J. Environ. Sci.* **2017**, *53*, 107–112.

(35) Tang, M.; Cziczo, D. J.; Grassian, V. H. Interactions of Water with Mineral Dust Aerosol: Water Adsorption, Hygroscopicity, Cloud Condensation, and Ice Nucleation. *Chem. Rev.* **2016**, *116* (7), 4205–4259.

(36) Sassine, M.; Burel, L.; D'Anna, B.; George, C. Kinetics of the Tropospheric Formaldehyde Loss onto Mineral Dust and Urban Surfaces. *Atmos. Environ.* **2010**, *44* (40), 5468–5475.

(37) El Zein, A.; Romanias, M. N.; Bedjanian, Y. Kinetics and Products of Heterogeneous Reaction of HONO with Fe2O3 and Arizona Test Dust. *Environ. Sci. Technol.* **2013**, *47* (12),

6325–6331.

(38) Bedjanian, Y.; Romanias, M. N.; El Zein, A. Uptake of HO_2 Radicals on Arizona Test Dust. *Atmos. Chem. Phys.* **2013**, *13* (13), 6461–6471.

(39) Gustafsson, R. J.; Orlov, A.; Badger, C. L.; Griffiths, P. T.; Cox, R. a.; Lambert, R. M. A Comprehensive Evaluation of Water Uptake on Atmospherically Relevant Mineral Surfaces: DRIFT Spectroscopy, Thermogravimetric Analysis and Aerosol Growth Measurements. *Atmos. Chem. Phys. Discuss.* **2005**, *5* (4), 7191–7210.

(40) Navea, J. G.; Chen, H.; Huang, M.; Carmichel, G. R.; Grassian, V. H. A Comparative Evaluation of Water Uptake on Several Mineral Dust Sources. *Environ. Chem.* **2010**, *7* (2), 162–170.

(41) Rubasinghege, G.; Grassian, V. H. Role(s) of Adsorbed Water in the Surface Chemistry of Environmental Interfaces. *Chem. Commun. (Camb).* **2013**, *49* (30), 3071–3094.

(42) Schripp, T.; Fauck, C.; Salthammer, T. Interferences in the Determination of Formaldehyde via PTR-MS: What Do We Learn from M/z 31? *Int. J. Mass Spectrom.* **2010**, *289* (2–3), 170–172.

(43) Inomata, S.; Tanimoto, H.; Kameyama, S.; Tsunogai, U.; Irie, H.; Kanaya, Y.; Wang, Z. Technical Note: Determination of Formaldehyde Mixing Ratios in Air with PTR-MS: Laboratory Experiments and Field Measurements. *Atmos. Chem. Phys.* **2008**, *8* (2), 273–284.

(44) Herrmann, J.-M. Fundamentals and Misconceptions in Photocatalysis. *J. Photochem. Photobiol. A Chem.* **2010**, *216* (2–3), 85–93.

(45) Chapuis, Y.; Klvana, D.; Guy, C.; Kirchnerova, J. Photocatalytic Oxidation of Volatile Organic Compounds Using Fluorescent Visible Light. *J. Air Waste Manage. Assoc.* **2002**, *52* (7), 845–854.

(46) Styler, S. A.; Myers, A. L.; Donaldson, D. J. Heterogeneous Photooxidation of Fluorotelomer

508 Alcohols: A New Source of Aerosol-Phase Perfluorinated Carboxylic Acids. *Environ. Sci.*
509 *Technol.* **2013**, *47* (12), 6358–6367.

510 (47) Yao, H.; Feilberg, A. Characterisation of Photocatalytic Degradation of Odorous Compounds
511 Associated with Livestock Facilities by Means of PTR-MS. *Chem. Eng. J.* **2015**, *277*, 341–
512 351.

513 (48) Benoit-Marquié, F.; Wilkenhöner, U.; Simon, V.; Braun, A. M.; Oliveros, E.; Maurette, M.-
514 T. VOC Photodegradation at the Gas–solid Interface of a TiO2 Photocatalyst. *J. Photochem.*
515 *Photobiol. A Chem.* **2000**, *132* (3), 225–232.

516 (49) Kirchnerova, J.; Herrera Cohen, M. L.; Guy, C.; Klvana, D. Photocatalytic Oxidation of N-
517 Butanol under Fluorescent Visible Light Lamp over Commercial TiO2 (Hombicat UV100
518 and Degussa P25). *Appl. Catal. A Gen.* **2005**, *282* (1–2), 321–332.

519 (50) Peral, J.; Ollis, D. F. Heterogeneous Photocatalytic Oxidation of Gas-Phase Organics for Air
520 Purification: Acetone, 1-Butanol, Butyraldehyde, Formaldehyde, and M-Xylene Oxidation. *J.*
521 *Catal.* **1992**, *136* (2), 554–565.

522 (51) Blake, N. R.; Griffin, G. L. Selectivtty Control during the Photoassisted Oxidatlon of 1-
523 Butanol on Titanium Dioxide. *J. Phys. Chem.* **1988**, *92* (13), 5697–5701.

524 (52) Nimlos, M. R.; Wolfrum, E. J.; Brewer, M. L.; Fennell, J. a; Bintner, G. Gas-Phase
525 Heterogeneous Photocatalytic Oxidation of Ethanol: Pathways and Kinetic Modeling.
526 *Environ. Sci. Technol.* **1996**, *30* (10), 3102–3110.

527 (53) Ye, X.; Chen, D.; Gossage, J.; Li, K. Photocatalytic Oxidation of Aldehydes: Byproduct
528 Identification and Reaction Pathway. *J. Photochem. Photobiol. A Chem.* **2006**, *183* (1–2),
529 35–40.

530 (54) Hirakawa, T.; Daimon, T.; Kitazawa, M.; Ohguri, N.; Koga, C.; Negishi, N.; Matsuzawa, S.;
531 Nosaka, Y. An Approach to Estimating Photocatalytic Activity of TiO2 Suspension by

Monitoring Dissolved Oxygen and Superoxide Ion on Decomposing Organic Compounds. *J. Photochem. Photobiol. A Chem.* **2007**, *190* (1), 58–68.

(55) Mellouki, A.; Wallington, T. J.; Chen, J. Atmospheric Chemistry of Oxygenated Volatile Organic Compounds: Impacts on Air Quality and Climate. *Chem. Rev.* **2015**, *115* (10), 3984–4014.